Scientific Eminence Group

Journal of Chemical Reactions and Catalysis Research

Research Article

Open Access

JCRC@scientificeminencegroup.com

Study of Hydrogen Transfer Reactions within the Framework of the Non-Equilibrium Approach; $CH_4 + OH \rightarrow CH_3 + H_2O$ Reaction

Igor Romanskii*

Institut Himiceskoj Fiziki Imeni N N Semenova RAN Russian Federation, Moscow, Russia

*Corresponding Author

Igor Romanskii, Institut Himiceskoj Fiziki Imeni N N Semenova RAN Russian Federation, Moscow, Russia, E--mail: ceng37@yandex.ru

Citation

Igor Romanskii (2025) Study of Hydrogen Transfer Reactions within the Framework of the Non-Equilibrium Approach; CH_4+ OH → CH_3 + H_2O Reaction. J Chem Reac Catal Res 3(1): 101

Publication Dates

Received date: November 10, 2025
Accepted date: November 29, 2025
Published date: December 02, 2025

Abstract

A theoretical study of the gas-phase reaction $CH_4 + OH \rightarrow CH_3 + H_2O$ kinetics (energy calculation level CCSD (T)/6311++G**//B3LYP/631+G**) in the temperature range 200 – 2000 K was performed. A discussion is held within the framework of the non-equilibrium model, in which at the fixed C..O distance the tunneling H-atom and system reorganization processes occur simultaneously. Kinetic analysis, performed with regard to a promoting effect of C(H)..O bond oscillation and the lifetime of the collision complex, leads to a close agreement with experimental data.

Keywords: Methane, Hydroxyl Radical, Non-Equilibrium Model, Promoting Vibrations, Collision Complex Lifetime

1. Introduction

The reaction of methane with the hydroxyl radical (Eq. 1) has attracted the attention of researchers for decades due to the key role this reaction plays both in the balance of atmospheric methane and in hydrocarbon combustion processes.

$CH_4 + OH \rightarrow CH_3 + H_2O$ (1)

As a result of intensive experimental studies of the reaction, performed by different scientific groups in a wide range of temperatures, reliable kinetic data were obtained, characterized by mutual consistency: the equations recommended in the reviews of 1986 [1] (Eq. 2) and 2005 [2] (Eq. 3) lead to very close values of the rate constants.

$k(T) = 2.49.10^{-18} T^{2.13} \exp(-1230/T)$ 250 -2000 K (2)

$k(T) = 2.27.10^{-18} T^{2.18} \exp(1350/T)$ 250 -2400 K (3)

in cm^3 molecule $^{-1}$ s^{-1}

Recent theoretical studies have been aimed at high-level calculation of the full-size PES of the reaction [3-5] and description of its kinetics both regard to the variational TST with correction for tunneling [6, 7] and using dynamic modeling [4, 6, 8-10] (only a few references are given).

The present work continues the study of gas-phase reactions of hydrogen atom transfer within the framework of the non-equilibrium approach. Previously, an attempt was made to use the data on the kinetics of reactions of the methyl radical with methane [11] and methanol (along the C–H [12] and O–H [13] bonds) to describe hydrogen atom tunneling dynamic aspects [13, 14]. The present work is devoted to examining the system dynamics at the moment of reactant collision from this point of view.

2. Theory

The non-equilibrium theory of proton transfer in solution [15-18] is based on the generalized Franck-Condon principle (GFCP) [19]: during proton tunneling, heavy atoms of the system retain their positions[1]. As shown by the study of the reactions of the methyl radical with methane (Eq. 4) and methanol (Eqs. 5, 6), for H-atom transfer reactions in the gas phase, the factor of constancy of the distance between the H-donor and acceptor atoms, Q, during tunneling comes to the fore [13]. In the potential energy diagram (Fig. 1), this condition determines the motion of the reaction system along the abde route; sections ab and de correspond to the motion of the system along the minimum energy path (MEP) in the reactant and product valleys, respectively, and section bd corresponds to the tunneling of the H-atom; at a fixed distance Q, tunneling occurs in a double-well potential $V(Q;r)$, where r is the tunneling coordinate[2].

$CH_4 + CH_3 \rightarrow CH_3 + CH_4$ (4)

$CH_3OH + CH_3 \rightarrow CH_2OH + CH_4$ (5)

$CH_3OH + CH_3 \rightarrow CH_3O + CH_4$ (6)

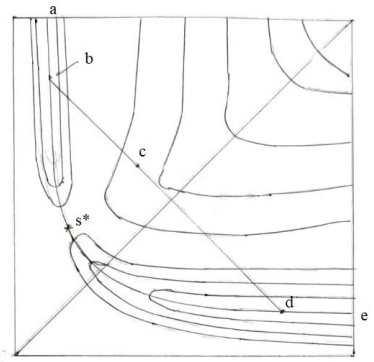

Figure 1: The route of the system in the non-equilibrium reaction of H-atom transfer. Comments in the text.

[1]It would probably be more accurate to talk about the unchanged system structure.

[2]For reaction (1) Q is the distance C…O at the moment of closest approach of the reactants; r is the distance C-H.

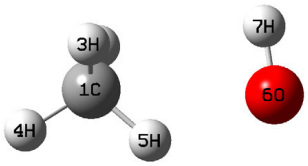

Scheme 1

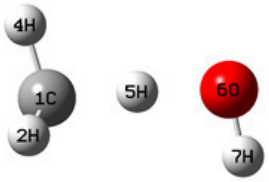

Scheme 2

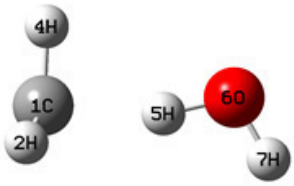

Scheme 3

The system structures at the characteristic points of the potential $V(r;Q)$. $D(H_4COH_7)= 180^o$, $Q= 2.6$ A; $r_{01} = 1.1$ A (Scheme 1), $r_b = 1.29$ A (Scheme 2), $r_{02} = 1.64$ A (Scheme 3).

It is easy to show the difference between this method of the reaction description and that one adopted in the classical TST and modern dynamic models. Let us imagine that at point b (Fig. 1) the system has some excess kinetic energy. If this is the translational energy of the relative motion of the reactants, the further development of the reaction will occur according to a dynamic scenario: the system can pass through the saddle point (SP), s^*, or tunnel through the equilibrium energy barrier on the way to it. On the other hand, if the entire excess kinetic energy at point b is transformed into the C-H bond vibrational energy, the system is able to pass to the final state as a result of tunneling of the H atom from some excited vibrational level of the double-well potential $V(Q;r)$.

In studying reactions (1) – (3), two models of H-atom tunneling were considered [13]. In model 1, it is assumed, in accordance with the GFCP, that the proton transition itself is preceded by symmetrization of the potential $V(Q;r)$. At this stage, the system shifts along the coordinate r (which is considered in this case as the structural coordinate of the reaction (coordinate ρ)) to a certain point c (Fig. 1); following this (slow) stage, at fixed distance Q and structure of the system, a fast tunnel transition of hydrogen from the left well of the potential $V(r; \rho^*,Q)$ (ρ^* is the value of the coordinate ρ at point c) to the right one occurs. This model describes well the kinetics of the symmetric reaction of methane with the methyl radical (Eq. 4). For the description of the asymmetric reactions of the methyl radical with methanol (Eq. 5 and 6), model 2, in which the processes of H-atom tunneling and system reorganization are considered to occur simultaneously, turned out to be more adequate[3]; the tunneling potential in this case is the asymmetric potential $V(Q;r)$. It is assumed that the transition from model 1 to model 2 is associated with a tunneling process slowdown in the asymmetric potential (see Section 4.2).

[3]In case of reaction 6, model 2 is not fully realized.

Regardless of the tunneling model, the equation used to describe the thermal rate constant of the reaction, $k(T)$, is:

$$k(T) = \sigma \int k(Q)dQ = \sigma \int \nu_t(Q,T)exp[-\Delta G^{*}(Q)/RT]dQ \quad (7a)$$

$$\Delta G^{*}(Q) = \Delta H^{*}(Q) - T\Delta S^{*}(Q) \quad (7b)$$

$$\Delta H^{*}(Q) = E_a + \Delta h^{*}(Q) \quad (7c)$$

$$\Delta S^{*}(Q) = 1000\{[\Delta h^{*}(Q) - \Delta g^{*}(Q)]/T\} \quad (7d)$$

$$\Delta h^{*}(Q) = h^{*}(Q) - h;\ \Delta g^{*}(Q) = g^{*}(Q) - g \quad (7e)$$

where σ is the symmetry number; ν_t is the tunneling frequency in the symmetric potential $V(r;Q,\rho^{*})$, ΔG^{*}, ΔH^{*} and ΔS^{*} are the free energy, enthalpy and entropy of activation, respectively, Δh^{*} and Δg^{*} are the thermal corrections to the enthalpy and the free activation energy, respectively, where $h^{*}(h)$ and $g^{*}(g)$ are the corresponding thermal corrections for the AC (reagents); R is the gas constant. The calculation of thermodynamic parameters is performed in the rigid rotor approximation without accounting for free and internal rotations of the AC and reactants.

To calculate the tunneling frequency $\nu_t(Q,T)$ the following relations are used:

$$\nu_t(Q,T) = \nu^{t\,00}(Q) + \Sigma_i\ \nu_t^{i}(Q,T) \quad (8a)$$

$$\nu_t^{i}(Q,T) = \nu_t^{ii}(Q)\ exp(-\Delta V_{i0}(Q)/RT) \quad (8b)$$

Here ν_t^{00} and ν_t^{ii} are the H-atom tunneling between zero and i-th levels of the double-well potential $V(r;\rho^{*},Q)$, respectively, and ΔV_{i0} is the energy difference between the i-th and zero levels of the potential.

3. Calculation Details

All calculations were performed using the Gaussian 03 software package [20] at the energy calculation level CCSD (T)/6-311++G**// B3LYP/6-31+G**. Calculations related to the determination of tunneling frequencies were performed on the basis of model 2. This is due, as already noted, to the preference of this model for the case of asymmetric reactions, on the one hand, and to the impossibility of performing calculations on the basis of model 1, on the other hand. The reason for this is an extremely high dependence of the system geometry on the structural coordinate ρ, which does not allow fixing the symmetrization point of the tunneling potential.

When optimizing the geometry for the key points of the equilibrium potential $V(Q;r)$: the positions of the left (r_{01}) and right (r_{02}) minima, as well as the barrier top (r_b) (schemes 1-3), along with the distance Q, the dihedral angle H_1COH_7 was also fixed (at a value of 180°). The values of r_{01} and r_{02} were taken to be equal to 1.1 and Q - 0.96 A, respectively.

The tunneling frequencies were calculated in the WKB approximation using the Brickman method [21, 22]. The calculations by Eq. 8 are carried out at i≤8. When calculating the thermo-chemical quantities, fixing the above geometric parameters of the system usually leads to the appearance of several (from one to three) imaginary frequencies, which, as assumed, reflects a change in the shape of the vibration potential, namely from a single-well potential to a double-well one. When determining the h^{*} and g^{*} values, the imaginary frequency values were replaced by the corresponding real ones.

The values of the CH_3 fragment umbrella vibration frequency, ν(CH_3), as well as the C(H)..O bond vibration frequency, ν(CO), in the collision complex (in the left well of the $V(r;Q)$ potential, Scheme 1), were calculated using the GaussView program in the process of calculating thermo-chemical h^{*} and g^{*} parameters.

The procedure for calculating individual parameters (y) included in the integrand of Eq. 7a consisted of two stages. In the first stage, the y values were calculated for the studied range of distances Q with a step of 0.1 Å. In the second stage, using the graphically determined dependence $y(Q)$ (in the form of polynomials of various degrees), the y values were obtained with a step of 0.025 Å. The greatest data scatter was observed when calculating the g^{*} values; this required excluding the most deviating g^{*} values when establishing the dependence $y(Q)$, thus limiting the number of variables.

4. Results and Discussion

4.1. Geometrical and Energetic Characteristics of the Reaction; Thermo-Chemical Calculations

The results of calculating the reaction energy, ΔE_{00}, and the barrier height at the saddle point, E_b^{SP}, are given in Table 1. At the selected calculation level, the difference between the found parameter values and the corresponding data from high-level calculations [4] is 2.0 – 2.5 kcal.mol^{-1}.

For model 2, the energy E_a is an equilibrium value determined by the energy expenditure in the section ab (Fig. 1), E_a^{eq}:

$$E_a = E_a^{eq}, \quad (9)$$

The values of the electron energy E_a and the barrier height E_b for the range of distances Q from 2.5 to 3.0 A are given in Table 2; the position of the barrier top on coordinate r, is also given there.

Table 3 demonstrates the changes in the system geometry, the value of the planar angle CH_5O (see Schemes) depending on the Q distance and the H-atom position on coordinate r.

The results of the thermo-chemical calculations are given in the Appendix (Tables 1S – 5S).

Table 1. Reaction energy, ΔE_{00}, and barrier height at saddle point, E_b^{SP} (kcal. mol^{-1})

Parameter	This work [a)]	[4] [b]
ΔE_{00}	10.91	-13.3
E_b^{SP}	8.52	6.4

a) CCSD (T)/6-311++G**//B3LYP/6-31+G**; b) analytical PES fitted ab initio data (PES-2014).

Table 2: Electronic activation energy E_a, height of direct (E_{b1}) and reverse (E_{b2})[a)] barriers; the barrier top on the r coordinate (r_b)

Q, A	E_a	E_{b1}	E_{b2}	r_b, A
2.5	4.216	4.331	11.225	1.205
2.6	2.805	6.572	15.15	1.29
2.7	1.823	10.168	19.979	1.36
2.8	1.146	14.634	25.336	1.419
2.9	0.675	19.708	31.021	1.479
3	0.339	25.165	36.866	1.537

a) Energy values in kcal.mol^{-1}

4.2. Tunneling of the H-atom [13, 14]

The description of the H-atom tunneling dynamics in the potential $V(r;Q)$ is associated with the concept of tunneling time, τ_t [23] . In this regard the WKB Buttiker and Landauer equation [24] for the tunneling time of a particle in a symmetric double-well potential $V(r)$ was used as the basis:

$$\tau_{sim} = \int_a^b \{0.5\, m/[V(r) - V_i]\}^{0.5}\, dr \quad (10)$$

(V_i is the energy of the ith vibrational level and m is the reduced mass of the particle).

Based on the results of kinetic calculations for reactions (4) – (6), it was suggested that in the case of an asymmetric potential barrier, the expression for the tunneling time should be corrected for the asymmetry factor η used in the Brickman WKB model [21, 22]:

$$\eta = [1 + (\pi \Delta V_{min} / h\nu_0)^2 T^{-2}]^{-0.5} \quad (11)$$

where ΔV_{min} is the difference in the energies of the minima in the potential $V(r;Q)$, ν_0 is the zero-point frequency of the H atom vibration in the left well of the potential, and T_{tr} is the transmission coefficient:

$$T_{tr} = exp\{-2\pi(2m)^{0.5} h \int_a^b [V(r) - Vi)^{0.5}\, dr\} \quad (12)$$

According to this assumption, the tunneling time of an H atom in an asymmetric potential $V(r;Q)$ should be described by the equation

$$\tau_t = \tau_t'/\eta \qquad (13)$$

where τ_t' is the tunneling time in the potential $V(r;Q)$ without taking into account the value of η.

In the case of the exothermic reaction of methane with the hydroxyl radical, the value of τ_t was calculated for the zero level in the left well of the $V(r;Q)$ potential and for the distance Q corresponding to the maximum of the rate constant $k(Q)$ (Eq. 7a), Q_m.

For this reaction (as for reactions (4)–(6)) the main change in the structure of the system is associated with the transition of the C atom from the sp^3 to the sp^2 state. Accordingly, the following parameter can be used as a criterion for the dynamic behavior of the system during the tunneling of the H atom:

$$n = \tau_t / T_{0.5} \qquad (14)$$

where $T_{0.5}$ is the half-period of the umbrella oscillation of the CH_3 fragment in the left well of the potential $V(r;Q)$; the $T_{0.5}$ value defined by the $\nu(CH_3)$ value (Section 3).

The τ_t, $T_{0.5}$ and n values calculation results are given in Table 4. The acquired value of n (> 1) is in agreement with the assumption that in an asymmetric potential the tunneling time of the H atom is relatively (compared $T_{0.5}$) large; in accordance with model 2, this enables the system structure to adapt to the H-atom motion. The latter implies in this case a significant change in the CH_5O angle (Schemes 1 – 3, Table 3).

Table 3: The angle CH_5O values (degrees) at the characteristic points of the potential V(r;Q)[a)]

Q,A	r_{01}	r_b	r_{02}
2.5	113.6	174	160.6
2.6	119.4	177.2	163.2
2.7	125	177.9	165.1
2.8	130.7	178.4	166.5
2.9	136.3	178.5	167.7
3	141.9	178.6	168.2

a) r_{01} = 1.1 A; r_{02}=Q-0.96 A; r_b (see Table 2)

Table 4: Calculation of the H-atom tunneling time, τ_t, and the half-period of CH_3 fragment umbrella vibration, $T_{05;}$ n=τ_t/T_{05}

Q, A	τ_t', s	η	τ_t, s	$\nu(CH_3)$, cm^{-1}	$T_{0.5}$, s	n
2.6	4.2(-15)	0.0865	4.85(-14)	1314	1.27(-14)	3.82

4.3. Kinetics and Mechanism of the Reaction

4.3.1. Calculation of the Rate Constant within the Framework of the Initial Model

The calculation results of thermal rate constants of the reaction obtained by Eq. 7 are presented in Table 5 (column 2) and Fig. 2 (curve 1). With the exception of the region of high (1500 – 2000 K) temperatures, theoretical values are three to six times lower than the experimental ones (Table 5, columns 9, 10) and Fig. 2 (curve 7).

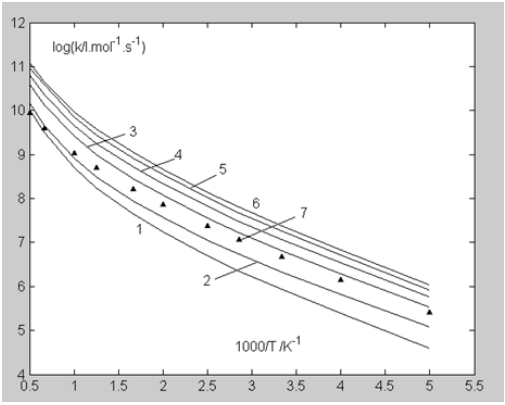

Figure 2: Thermal rate constant for reaction CH_4 + OH. Without promoting (curve 1); with promoting (given C…O bond promoting vibration levels): zero (curve 2), zero and first (curve 3), zero – second (curve 4), zero – third (curve 5), zero – fourth (curve 6); experiment [1] (curve 7).

Table 5: Thermal rate constants (l.mol^{-1}.s^{-1})[a]

T, K	Theory							Experiment	
	k	k_0	k_1	k_2	k_3	k_4	k_1'	[1]	[2]
2000	1.02(10)	1.43(10)	3.84(10)	6.32(10)	9.27(10)	1.17(11)	8.27(9)	8.73(9)	1.09(10)
1500	3.10(9)	4.60(9)	1.32(10)	2.24(10)	3.84(10)	4.35(10)	3.45(9)	3.86(9)	4.66(9)
1000	5.01(8)	8.29(8)	2.59(9)	4.53(9)	7.14(9)	9.31(9)	8.85(8)	1.08(9)	1.23(9)
800	1.70(8)	3.03(8)	9.78(8)	1.74(9)	2.79(9)	3.72(9)	3.88(8)	4.94(8)	5.39(8)
600	4.48(7)	8.77(7)	2.85(8)	5.15(8)	8.26(8)	1.11(9)	1.37(8)	1.60(8)	1.64(8)
500	1.75(7)	3.65(7)	1.18(8)	2.15(8)	3.43(8)	4.63(8)	6.40(7)	7.22(7)	7.03(7)
400	5.00(6)	1.13(7)	3.59(7)	6.54(7)	1.03(8)	1.40(8)	2.26(7)	2.43(7)	2.20(7)
350	2.25(6)	5.36(6)	1.66(7)	3.02(7)	4.73(7)	6.37(7)	1.15(7)	1.17(7)	1.02(7)
300	8.54(5)	2.16(6)	6.49(6)	1.17(7)	1.80(7)	2.40(7)	4.95(6)	4.71(6)	3.81(6)
250	2.46(5)	6.71(5)	1.92(6)	3.41(6)	5.13(6)	6.74(6)	1.66(6)	1.41(6)	1.04(6)
200	3.98(4)	1.23(5)	3.31(5)	5.76(5)	8.43(5)	1.08(6)	3.31(5)	2.56(5)	1.66(5)

a) k – calculation by Eq. 7, k_0 – k_4 – taking into account C…O vibration (the index corresponds to the upper vibration level involved in the reaction (starting from the zero level) explanation in the text), k_1' – rate constant k_1 with correction for the lifetime of the collision complex (Eq. 21).

4.3.2. The Promoting Effect

In studies devoted to proton transfer reactions in solution, the heavy atoms vibration of the three-center subsystem A(H)..B is considered as one of the promoting factors [25]. Assuming that this mechanism retains its significance for the reaction in the gas phase (see the next Section), we took as an initial condition that C(H)..O bond five vibrational levels participate in the reaction: the zero and four next excited ones. The immediate cause of the reaction acceleration is the decrease in the tunneling distance achieved during the vibration of the C… O bond: the initial tunneling point b (distance Q) shifts to the position b_0 (distance Q_0) for the zero vibrational level, b_1 (distance Q_1) for the first level and so on (Fig. 3). The promoting factor, $F_j(Q)$, for a given distance Q and vibrational level j is determined by the relation:

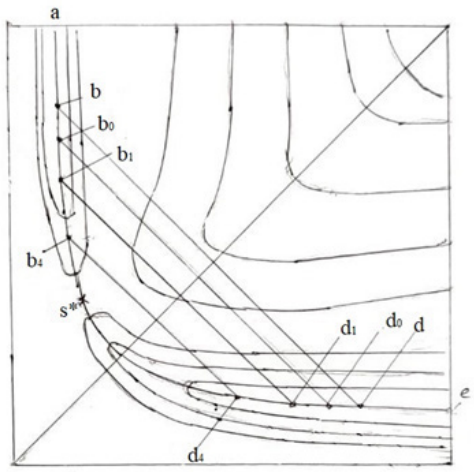

Figure 3: The influence of C...O vibrations in the collision complex on the system route in the reaction CH_4 + OH: comments in the text.

$$F_j(Q) = v_t(Q_j)v_t(Q)^{-1} \{exp\{-[E_j(Q) - E_0(Q)]/RT\} \quad (15)$$

where $v_t(Q)$ and $v_t(Q_j)$ are the tunneling frequencies of the H-atom tunneling at distances Q and Q_j, respectively; $E_0(Q)$ and $E_j(Q)$ are the energies of the zero and j vibrations at point b.

The rate constant value $k(Q)$ taking into account promotion, $k_{pr}(Q)$, was obtained from the relation

$$k_{pr}(Q) = k(Q)\, F(Q) \quad (16)$$

where $F(Q)$ is the promotion factor for a given Q:

$$F(Q) = \Sigma_j F_j(Q) \quad (17)$$

By substituting the $k_{pr}(Q)$ value into Eq. 7a, the resulting value of the thermal rate constant, k_{pr}(T), was determined.

$$k_{pr}(T) = \int_Q k_{pr}(Q)\, dQ \quad (18)$$

The calculations according to Eqs. (15) – (18) were based on the energy profile of the system along the MEP, presented as a dependence on Q, $V(Q)$, the corresponding dependence for the frequency v_t, $v_t(Q)$, and the energy $E_0(Q)$, determined by the ν(CO) values (Section 3). When calculating the $E_j(Q)$ values, the distance between neighboring vibrational levels, $\Delta E_{j,j+1}(Q)$, was considered equal to twice the value of $E_0(Q)$: $\Delta E_{j,j+1}(Q) = 2\, E_0(Q)$. The Q_j values for the $v_t(Q_j)$ function (Eq. 15) were found using the inverse $V(Q)$ dependence $Q(V)$ and the energies $E_j(Q)$. In general, the number of vibrational levels in the equation grows up with increasing interval $Q - Q_{min}$, where Q_{min} (= 2.5 A) is the minimum value of Q available for calculation.

The values of $E_0(Q)$ are given in Table 6. Table 7 provides, as an example, the calculation details of the values of $F_j(Q)$, $F(Q)$ and $k_{pr}(Q)$ at T=500 K and Q=2.8 A. Fig. 4 demonstrates the rate constant $k(Q)$ changes at T=500 K depending on the number of C(H)…O vibrational levels j participating in the reaction.

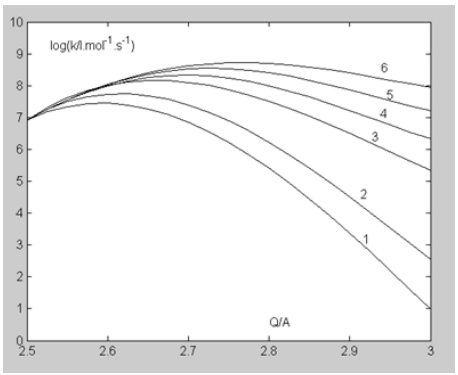

Figure 4: Reaction rate constant $k_{pr}(Q)$ (Eq. 16) at T = 500 K as a function of C…O bond promoting vibration levels (curve number in parentheses): zero (2), zero and first (3), zero – second (4), zero – third (5), zero – fourth (6); $k(Q)$ in Eq. 7 (1).

Table 6: Zero level energy (E_0) and period (T_{col}) of C(H)..O vibrations

Q, A	E_0		$T_{col}\,10^{-13}$, S^{-1}
	cm^{-1}	$kcal.mol^{-1}$	
2.5	304.9	0.436	1.09
2.6	255.9	0.365	1.3
2.7	213.8	0.306	1.56
2.8	177.5	0.254	1.88
2.9	148.4	0.212	2.25
3.0	132	0.188	2.52

Table 7: Calculation $F_j(Q)$, $F(Q)$ and $k_{pr}(Q)$ values (Eqs. 15 -18); T=500 K Q=2.8 A, $\nu_t(Q)$=3.68(9) s^{-1}, k(Q)=2.64(5) $l.mol^{-1}.s^{-1}$

j	E_j, $kcal.mol^{-1}$	Q_j, A	$\nu_t(Q_j)$	f_j a)	P_j b)	$F_j(Q)$	$F(Q)$	$k_{pr}(Q)$
0	0.254	2.759	2.47(10)	6.7	1	6.7	6.7	1.764(6)
1	0.762	2.661	1.06(12)	287	0.464	133.3	140	3.688(7)
2	1.27	2.611	4.58(12)	1244	0.279	346.6	487	1.282(8)
3	1.778	2.57	1.19(13)	3235	0.167	540.4	1027	2.706(8)
4	2.286	2.534	2.24(13)	6094	0.1	610.6	1638	4.314(8)

a) $f_j = \nu_t(Q_j)/\nu_t(Q)$; b) $P_i = exp\{-[E_j(Q) - E_0(Q)]/RT\}$

In the plot for the thermal rate constant (Fig. 2), an increase in the number of vibrational levels involved in the reaction leads to the kinetic curve upward shift; as a result, the entire region of the experimental rate constant is covered. At the same time, the course of the change in the experimental dependence (curve 7) retains a noticeable difference from those predicted by the calculation: at low temperatures, curve 7 is close to curve 3 (the zero and first vibration levels participate in the reaction), and at high temperatures, to curve 1 (there is no promotion). In the next section, the observed behavior of the experimental dependence is considered in connection with the lifetime of the collision complex.

4.4. Collision Complex Lifetime (τ_{lf})

The Bunker equation [26], obtained on the basis of real gases physical properties, predicts a decrease in the τ_{lf} value with temperature:

$$\tau_{lf} = 1.50\ \sigma\ \mu^{1/2}\ \varepsilon^{1/6}\ (2k_BT)^{-2/3} \qquad (19)$$

Here σ is the collision diameter, ε is the well depth for the Lennard-Jones potential, μ is the reduced mass of the complex, and k_B is the Boltzmann constant. The values of the σ and ε parameters for the reaction collision complex were obtained on the basis of tabulated values for the reactants [see, for example, [27]): σ as the arithmetic mean, and ε as the geometric mean (Table 8)[4]. As the calculation shows, in the temperature range from 200 to 2000 K, the τ_{lf} value changes from 4.1 to 1.0. 10^{-13} sec (Table 9). For comparison, the oscillation period of the C(H)...O bond, T_{vb}, at Q= 2.6 A (corresponding to the maximum of the k (Q) value at all temperatures) is $1.3.10^{-13}$ sec. Accordingly, with increasing temperature the ratio $p = \tau_{lf}/T_{vb}$ changes from 3.5 to less than 1 (Table 9). These changes are in obvious agreement with the transition from the promotion to its complete absence described in the previous section.

The variable parameter f (Table 9) shows the change in lifetime relative to its value at 200 K:

$$f = \tau_{lf}/\tau_{lf}(200\ K) \qquad (20)$$

[4]At first glance, there is an obvious contradiction between the small value of the well depth ε for the complex (Table 8) compared to the significantly higher values of the energies of the zero (Table 6) and first (Table 7) levels of the C(H)..O bond vibrations. The explanation may apparently be that the promoting vibrations of the C(H)..O bond are directed not strictly along the MEP, but at some angle to it.

Table 8: σ and ε values

	σ ,cm	ε,cm^{-1}
CH_4	3.41	14.9
OH	2.66	19.9
$H_3C(H)\ldots OH$	2.86	17.22

Table 9: Collision lifetime τ_{lf} (Eq. 16); $p= \tau_{lf}/T_{col}$ [a)] and $f= \tau_{lf}/\tau_{lf}$ *(200 K)* ratios

T, K	$\tau_{lf}10^{-13}$, S	*p*	*f*	T, K	$\tau_{lf}10^{-13}$, S	*p*	*f*
2000	0.97	0.75	0.215	400	2.85	2.19	0.63
1500	1.18	0.91	0.261	350	3.12	2.40	0.689
1000	1.55	1.19	0.342	300	3.45	2.66	0.763
800	1.8	1.38	0.397	250	3.9	3.00	0.862
600	2.18	1.67	0.481	200	4.52	3.48	1
500	2.46	1.89	0.543				

a) Here T_{col} ($1.3.10^{-13}$ s) is period of C...O collision at 2.6 A.

The rate constant k_1 adjusted for this correction, k_1' (Eq. 21), shows a close agreement with the experiment for the entire studied temperature range (Fig. 5, Table 5).

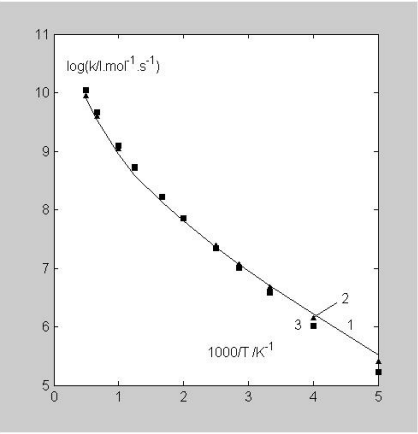

Figure 5: Thermal rate constant for reaction CH_4 + OH: calculation using Eq. 21 (curve 1); experiment: [1] (curve 2) and [2] (curve 3).

$k_1' = k_1 f$ (21)

The direct influence of the collision complex lifetime on the reaction rate observed in this case apparently reflects a change in the population of the C(H)…O bond vibrational levels.

Thus, the performed kinetic analysis allows us to identify several dynamic characteristics of the reaction:

(1) The process of H-atom tunneling at a fixed C...O distance occurs with simultaneous reorganization of the system.

(2) The reaction process occurs with the formation of a collision complex;

(3) The motion of the system along the MEP occurs both due to the translational energy of the reagents and due to vibrations of the C (H)..O bond;

(4) Two vibrational levels of the C (H)..O bond mainly participate in the reaction: zero and first ones;

(5) When temperature increases, the promoting effect of vibration is limited by of the collision complex lifetime.

Taking into account the insufficient accuracy of some calculations (Sections 3 and 4.1), it appears that the observed agreement between theory and experiment for the thermal rate constants (Fig. 5 and Table 5) should be partly attributed to the mutual compensation of calculation errors. It seems, however, that the obtained results are significant and in total confirm the realism of the non-equilibrium approach to studying the gas phase H-atom transfer reactions.

References

1. D L Baulch, et al. (1986) Evaluated kinetic data for high--temperature reactions. Volume 5. Part 1. Homogeneous gas phase reactions of the hydroxyl radical with alkanes, J. Phys. Chem. Ref. Data 15: 465-592.

2. DL Baulch, et al. (2005) Evaluated kinetic data for combustion modeling: Supplement II, J. Phys. Chem. Ref. Data, 34: 757 – 1397.

3. BJ Lynch, PL Fast, M Harris, DG Truhlar (2000) Adiabatic connection for kinetics, J. Phys. Chem. 104: 4811-19.

4. J Espinosa-Garcia, JC Corchado, (2015) QCT dynamics study of the reaction of hydroxyl radical and methane using a new ab initio fitted full-dimensional analytical potential energy surface, Theor. Chem. Acc. 134: 6.

5. J. Li, H Guo, (2015) Communication: An accurate full 15 dimensional permutationally invariant potential energy surface for the OH + CH_4→ H_2O + CH_3 reaction, J. Chem. Phys. 143: 221103

6. YV Suleimanov, J Espinosa-Garcia (2016) Recrossing and tunneling in the kinetics study of the OH + CH_4→ H_2O + CH_3 reaction, J. Phys. Chem. B 120: 1418-28.

7. J Li, K Guo (2018) Thermal rate coefficients and kinetic isotope effects for the reaction OH + CH_4→ H_2O + CH_3 on an ab initio-based Potential Energy Surface, J. Phys. Chem. A 122: 2645-52

8. JW Allen, et al. (2013) Communication: Full dimensional quantum rate coefficients and kinetic isotope effects from ring polymer dynamics for a seven-atom reaction OH + CH_4→ CH_3 + H_2O, J. Chem. Phys. 138: 221103.

9. H. Song, et al. (2014) Effects of reactant rotation on the dynamics of the OH + CH_4→ H_2O + CH_3 reaction: A six-dimensional study, J. Chem. Phys. 140: 084307.

10. J Espinosa-Garcia, J C Corchado (2016) Product translational and vibrational distributions for the OH/OD + CH_4/CD_4 reactions from quasiclassical trajectory calculations. Comparison and experiment, J. Phys. Chem. B 120: 1446-53.

11. IA Romanskii (2022) Study of gas-phase reactions within the modified Marcus model. IV. Arrhenius equation for the reaction CH_4 + CH_3 → CH_3 + CH_4, Reaction Kinetics, Mechanisms and Catalysis 135: 2401-23.

12. IA Romanskii (2023) Study of gasphase reactions within the modified Marcus model. V. Arrhenius equation for the reaction CH_3OH + CH_3 → CH_2OH + CH_4, Univers J. Catal. Sci. 1: 110-130.

13. IA Romanskii (2024) Investigation of methyl radical with methane and methanol reactions in the framework of a non-equilibrium approach; dynamic aspect, Comp. and Theor. Chem. 1239: 114725.

14. IA Romanskii (2025) Corrigendum to "Investigation of methyl radical with methane and methanol reactions in the framework of a non-equilibrium approach; dynamic aspect", Comp. and Theor. Chem. 1253: 115408.

15. RA Marcus (1957) On the theory of oxidation - reduction reactions involving electron transfer. II. Applications to data on the rates of isotopic exchange reactions, J. Chem. Phys. 26: 867–71.

16. RA Marcus (1968) Theoretical relations among rate constants, barriers and Broensted slopes of chemical reactions, J. Phys. Chem. 72: 891-99.

17. VG Levich, RR Dogonadze, ED German, et al. (1970) Theory of homogeneous reactions involving proton ransfer, Electrochimica Acta 15: 353–67.

18. ED German, RR Dogonadze (1977) Quantum-mechanical theory of the kinetics of proton transfer reactions, Supplement to R. P. Bell, The proton in chemistry, Mir, Moscow: 350–76.

19. RR Dogonadze, AM Kuznetsov (1974) Theory of the elementary act of charge transfer reactions in polar solvents, Mendeleev Chem. J. 19: 242–50.

20. MJ Frisch, GW Trucks, HB Schlegel, GE Scuceria, et al. (2004) Gaussian 03. (Revision C.02), Gaussian Inc., Wallingford CT.

21. J Brickmann, in: P Schuster, G Zandel, C Sandorfy (1976) Proton Motions in Hydrogen Bond – Recent Developments in Theory and Experiments. North-Holland Publishing Co.,

Amsterdam: 217–43.

22. MM Szczesniak, S Scheiner (1985) Effects of external ions on the dynamics of proton transfer across a hydrogen bond, J. Phys. Chem. 89: 1835–40.

23. K Maji, CK Mondal, SP Bhattacharyya (2007) Tunneling time and tunneling dynamics, International Reviews in Physical Chemistry 26: 647-70.

24. M Buttiker, R Landauer (1982) Traversal Time for Tunneling, Phys. Rev. Lett. 49: 1739-42.

25. MV Bazilevsky, MV Vener (2003) Theoretical studies of proton and hydrogen atom transfer reactions in the condensed phase, Usp. Khim. 72: 1-33 [Russ. Chem. Rev. 72 (2003) (Engl. Transl.)].

26. DL Bunker (1960) Mechanics of atomic recombination reactions, J. Chem. Phys. 32: 1001–5.

27. AW Jasper, JA Miller (2014) Lennard-Jones parameters for combustion and chemical kinetics modeling from full-dimensional intermolecular potentials, Combust. Flame 161: 101-10.